Co-adsorption of Ammonium, Phosphate, Strontium and Arsenate from Contaminated Water by a Low Cost Biochar. Performance and Mechanisms

Despina Vamvuka*, George Asiminas, Antonios Stratakis, and Despina Pentari

Mineral Resources Engineering Department, Technical University of Crete, Chania, Greece
Email: dvamvouka@tuc.gr (D.V.); gasiminas@tuc.gr (G.A.); astratakis@tuc.gr (A.S.); dpentari@tuc.gr (D.P.)
*Corresponding author

Manuscript received December 17, 2024; revised February 10, 2025; accepted April 14, 2025; published May 19, 2025

***Abstract*—Co-adsorption of ammonium, phosphate, strontium and arsenate ions from polluted water sources by a low-cost nut residue biochar, without using any chemicals, was investigated. The adsorption behavior of biochar was examined for different experimental parameters and the mechanisms of adsorption were explored through structural, mineralogical and chemical analyses, as well as modeling of experimental data. At equilibrium, a higher ionic strength favored the adsorption process, whereas the uptake of each ion by the solid increased significantly when all ions co-existed in the solution, implying no competition between them for sorption sites. The experimental data were fitted with great accuracy by the Freundlich isotherm model. The maximum adsorption capacity of the biochar achieved for ammonium, phosphate, strontium and arsenate was 50.3 mg/g, 121 mg/g, 66.9 mg/g and 62.9 mg/g, respectively. The potential mechanisms of adsorption were the chemical complexation of all ions with the adsorbent, electrostatic attraction for ammonium and strontium cations, ligand exchange for phosphate and arsenate ions and mineral surface precipitation for phosphate, strontium and arsenate ions.**

***Keywords*—co-adsorption, ammonium, phosphate, strontium, arsenate, biochar**

I. Introduction

Water is an essential resource for all living organisms and ecosystems and its contamination has severe consequences for human health and the environment. Among the numerous pollutants, ammonium and phosphate can enter water systems from various sources, the most important of which are municipal and industrial wastewaters and excessive fertilizers, or fungicides and herbicides used in agriculture [1–3]. The migration of soluble ion forms from soil to water bodies, even at concentrations as low as 0.2 mg/L NH_4^+ and 0.02 mg/L PO_4^{3-} [4], can lead to eutrophication, by triggering bacterial growth and algal blooms, posing a serious threat to aquatic biodiversity and human health [5–8].

Heavy metals strontium and arsenic present in surface and ground waters at concentrations 0.01–0.02 mg/L are very toxic, leading to serious health issues to living beings [9]. Strontium is discharged from radioactive wastes and arsenic from lithogenic sources. Also, they are released into the environment from various industrial activities including the production of ceramics, glass, fireworks and fertilizers, as well as from coal mining, petroleum refining, agricultural processing and waste management practices [9, 10].

Effective techniques are crucial for removing NH_4^+, PO_4^{3-} and heavy metals Sr^{2+}, As^{5+} from water to protect ecosystems. Numerous methods have been developed to remove these pollutants from contaminated water sources including physical, chemical and biological approaches. While physical and chemical techniques are effective, they often involve high costs and complex operations, whereas biological methods generally require more time to be effective [1, 6, 8, 10, 11]. The adsorption process has emerged as a simpler, more efficient, eco-friendly and cost-effective solution. Various materials have been explored as adsorbents including active carbon, carbon nanotubes, graphene, zeolites, resins and clays [3, 6, 8, 10–13]. However, the high cost and challenges related to disposal or recovery hinder the widespread use of these adsorbents. As a result, attention has recently shifted toward lower-cost and widely available alternatives, such as biochar. Derived from the pyrolysis of various organic wastes, biochar has shown high adsorption capabilities, due to its large surface area, high porosity and cation exchange capacity. The presence of negatively charged functional groups on its surface favors the adsorption of cationic pollutants, however limits the adsorption of anionic ones [1–3, 6, 7, 9, 11, 14].

Ammonium, phosphate, or heavy metals rarely exist in isolation in the environment and often occur together in wastewater. The adsorption of these pollutants onto biochar is influenced by the biochar properties, process conditions and the competitive interactions between ions for available sorption sites. The simultaneous immobilization of NH_4^+, PO_4^{3-}, Sr^{2+} and As^{5+} by biochars has not been previously studied. Most investigations focused on the removal of ammonium and phosphate from binary systems. The adsorption capacities for ammonium and phosphate from a date palm biochar were reported 48 mg/g and 27.4 mg/g, respectively [13], while from sewage sludge-derived biochar 10 mg/g and 63.2 mg/g, respectively [15]. To enhance the adsorption effectiveness of biochars for ammonium and phosphate, several modification techniques have been developed. Magnesium-modified biochars from rice straw, soybean straw, pine bark and corn stalk showed maximum adsorption capacities for ammonium and phosphate between 0.7–177.2 mg/g and 1.4–253.9 mg/g, respectively [2, 7, 8, 16]. Also, when using magnesium-doped peanut shell biochar/bentonite composites, the maximum ammonium and phosphate adsorption capacities reached 39.5 mg/g and 132.2 mg/g, respectively [17]. On the other hand, the results from the application of different modifiers, such as iron [3], or calcium alginate [6], on agricultural or industrial waste biochars indicated lower adsorption capacities for ammonium 10.6 mg/g and 12.3 mg/g, respectively, or for phosphate 13.5 mg/g and 24.1 mg/g, respectively. As concerns strontium and arsenic, there is no literature data on their simultaneous adsorption from aqueous solutions. Biochars derived from agricultural byproducts have

demonstrated the ability to adsorb strontium or arsenic from single solutions, with maximum adsorption capacities ranging from 0.6–0.74 mg/g [18] and 0.8–7.1 mg/g [19, 20], respectively.

Previous studies in our lab have demonstrated that NH_4^+, PO_4^{3-}, Sr^{2+} and As^{5+} ions co-existed in wastewater from municipal solid waste and sewage sludge treatment units, as well as from agro-industrial enterprises [21]. Consequently, the aim of the current work was to investigate the co-adsorption of all the above ions by a low-cost nut residue biochar, without using any chemicals, as a novel approach. Given the lack of data in such multiple contaminants adsorption, this study could provide valuable information on the competitive effects of these pollutants for solid adsorption sites, leading to the improved design of biochar adsorbents for the treatment of wastewater. The adsorption behavior of biochar was examined for different experimental parameters and the mechanisms of adsorption were explored through structural, mineralogical and chemical analyses, as well as modeling of the experimental data.

II. Materials and Methods

A. Preparation of the Adsorbent and Characterization

The agro-industrial waste used for the simultaneous adsorption of ammonium, phosphate, strontium and arsenate ions, sourced by a private nut enterprise, almond husks (AH), was ground in a cutting mill to a particle size below 500 μm and then riffled in a Jones riffler to obtain homogeneous samples.

Activation of the raw material was carried out in a fixed-bed reactor unit, previously described in another study [22]. About 15 g of AH material was charged onto a grid basket within the reactor, which was sealed and placed into the furnace. After flushing with pure nitrogen for 0.5 h to eliminate air, the temperature controller was set to 700°C, a heating rate of 10°C/min and a retention time of 0.5 h. The temperature of the sample was monitored by a Cr-Ni-Cr thermocouple with a precision of ± 2°C. The flow rate of nitrogen was 200 mL/min. Following the activation of the sample by nitrogen, reagent gas was switched to steam by injecting distilled water at a flow rate of 0.5 mL/min, via an automatic syringe pump. A 2 m stainless steel pipe surrounding the reactor provided a uniform flow of steam. Activation by steam at 700°C lasted 1 h, after which the system was cooled under nitrogen. The activated biochar material from repeated experiments was homogenized and characterized as follows.

For proximate and ultimate analyses, high-temperature programmable furnaces, a thermal analysis system TGA/DTG-6 from Perkin Elmer and a Flash 2000 CHNS analyzer from Thermo Fisher Scientific Inc. were employed. For specific surface area and pore volume measurements, an Autosorb 1Q-C-MP analyzer from Quantachrome was used, after out-gassing the samples at 200°C under vacuum for 1 h. For identification of the chemical functional groups of the biochar before and after adsorption of the selected ions, a Spectrum 100 Fourier Transform Infrared (FTIR) spectrophotometer from Perkin Elmer was used. FTIR spectra were recorded in a wave number range of 400-4000 cm^{-1} with a resolution of 4 cm^{-1}.

An X-ray diffractometer (XRD), specifically the Bruker AXS S2 Ranger EPS model, was used to examine the mineral phases on the biochar surface before and after ions adsorption. The analysis was conducted within a 2–70° 2θ° scan range, with an increment of 0.02°/s. The Crystallography Open Database (COD) and DIFFRAC-Plus software were utilized to evaluate the spectra.

B. Kinetic and Adsorption Experiments of Ions

The reagents used to generate the various ions for adsorption were NH_4OH, KH_2PO_4, $Sr(NO_3)_2$ and $Na_2HAsO_4.7H_2O$ of analytical grade (Sigma-Aldrich Chemical Co.). A series of concentrations of 10, 50, 100, 200, 300 mg/L were prepared by distilled water dilution from the stock solutions of 1000 mg/L, for each ion. The pH of each solution was adjusted to an initial value of 7 by 0.1M HCl and 0.1M NaOH. The pH meter was a Toledo Metter model.

For the kinetic experiments, which were performed in order to determine the equilibrium contact time, 50 mg/L of NH_4^+ or PO_4^{3-} solution and 10 mg/L of Sr^{2+} or As^{5+} solution were mixed with 4 g/L of biochar material and stirred on a mechanical shaker at 200 rpm, at room temperature for 24 h. Liquid suspensions were withdrawn at specific contact times, filtered through micro-porous filters, analyzed for pH and subsequently for the residual concentration of each ion in the solution. The methods of nesslerization 3642-SC and vanadomolybdophosphoric 3655-SC, of Smart 3 colorimeter from LaMotte, were adopted for the measurements of NH_4^+ and PO_4^{3-} concentrations respectively, while an inductively coupled plasma mass spectrometer ICP-MS 7000cx from Agilent Technologies was adopted for the measurements of heavy metals Sr^{2+} and As^{5+}.

Following the establishment of equilibrium contact time, the adsorption experiments were conducted at the same experimental conditions and procedure as above, for all selected initial concentrations and for at least two replicates to ensure reproducibility of data (relative standard error RSE). The results reported below include the concomitant adsorption of NH_4^+ and PO_4^{3-} ions, as well as that of all ions studied NH_4^+, PO_4^{3-}, Sr^{2+} and As^{5+} and their comparison with single ion adsorption from recent investigations [22–24], for adsorbent doses of 4 g/L and 2 g/L (the experimental procedure is illustrated in Fig. A1).

C. Desorption Experiments of Ions

To access the desorption potential of biochar saturated with ions after adsorption, leaching experiments were conducted using only de-ionized water, to evaluate the release of ammonium and phosphate as nutrients for plant growth. 100 mg of spent material after adsorbing 100 mg/L of each ion was mixed with 200 mL of de-ionized water and agitated on a mechanical shaker at 200 rpm and room temperature for 72 h. Liquids were collected every 12 h, filtered and analyzed for ion concentration using the colorimeter and the ICP-MS spectrophotometer. The leaching rate of each ion was determined as follows:

$$LR(\%) = \frac{C \times V}{m_i} \times 100 \quad (1)$$

where C is the ion concentration (mg/L) at each specific time, V is the solution volume (L) and m_i is the weight of the ion (mg) in 100 mg of adsorbent used.

D. Modeling of Kinetic and Adsorption Experiments

For kinetic modeling, both the pseudo-first-order model

(Eq. 2) and the pseudo-second-order model (Eq. 3) were used, as they are widely recognized for providing consistent and accurate results [9, 10].

$$\log(q_e - q_t) = \log q_e - \frac{k_1}{2.303}t \quad (2)$$

$$\frac{t}{q_t} = \frac{1}{k_2 q_e^{\,2}} + \frac{t}{q_e} \quad (3)$$

To model the adsorption data, the Langmuir (Eq. 4) and Freundlich (Eq. 5) isotherms were utilized [10]. A linear approach was employed to calculate the isotherm constants.

$$\frac{C_e}{q_e} = \frac{1}{bC_e} + \frac{C_e}{Q} \quad (4)$$

$$\log q_e = \log k + \frac{1}{n}\log C_e \quad (5)$$

The adsorption performance was assessed using Eq. (6).

$$\%Ionremoval = \frac{C_0 - C_e}{C_0} x100 \quad (6)$$

The amount of metal adsorbed per unit mass of adsorbent (uptake), denoted as q (mg/g), was determined using Eq. (7):

$$q = \frac{(C_0 - C)V}{m} \quad (7)$$

where C_0 and C represent the initial and final concentrations of metal ions (mg/L) in the solution, V is the volume of the solution (L), and m is the mass of the adsorbent (g).

III. Results and Discussion

A. Characterization of Raw Material and Biochar

The physical and chemical properties of the raw material and the biochar produced after nitrogen/steam activation are indicated in Table 1. The raw material was lean in ash and rich in volatile matter, which was released during the thermal decomposition of the sample at 700°C. Thus the biochar consisted of higher carbon content, lower hydrogen content and undetectable concentrations of nitrogen and sulfur. However, the percentage of oxygen of the biochar remained at elevated levels, increasing its polar and hydrophyllic state [25]. Table 1 also shows that the specific surface area and pore volume of the material were increased by about 260 and 5 fold, respectively, after the thermal treatment of raw almond husks under a nitrogen/steam atmosphere.

Table 1. Proximate, ultimate and structural analyses of solid material (% dry, "-" below detection limits)

Sample	Volatiles	Fixed carbon	Ash	C	H	N	O	S	Specific surface area (m^2/g)	Micropore volume×10^2 (cm^3/g)
Almond husk raw (AH)	73.0	26.5	0.5	53.6	6.0	0.5	39.4	-	2.6	6.7
Almond husk biochar (AHB)	-	97.6	2.4	66.5	1.2	-	29.9	-	665	34.0

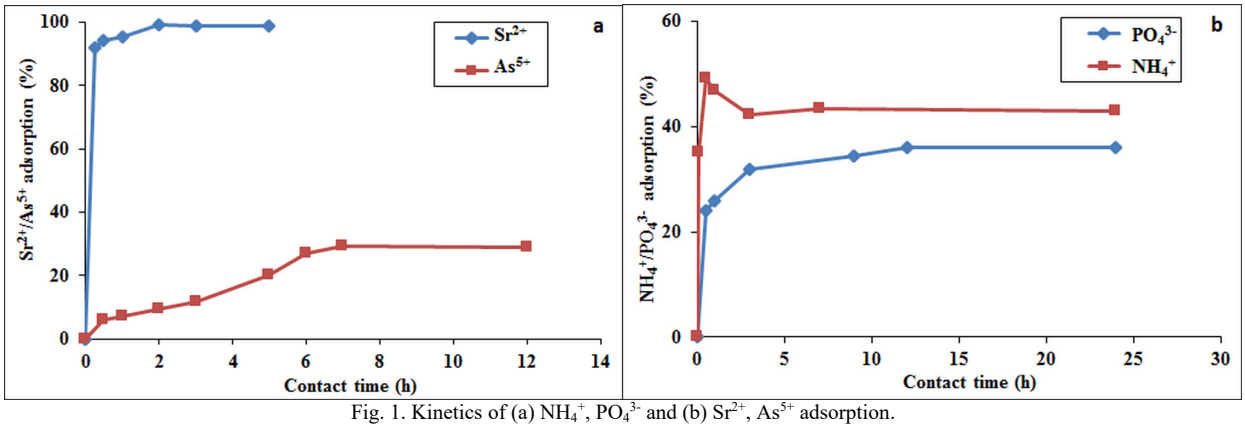

Fig. 1. Kinetics of (a) NH_4^+, PO_4^{3-} and (b) Sr^{2+}, As^{5+} adsorption.

Table 2. Kinetic model parameters of NH_4^+, PO_4^{3-}, Sr^{2+}, As^{5+} ions adsorption

	Kinetic model parameters					
	Pseudo-first order			Pseudo-second order		
	q_e (mg/g)	k_1 (1/h)	R^2	q_e (mg/g)	k_2 (1/h)	R^2
NH_4^+	1.030	0.002	0.738	3.780	0.260	0.997
PO_4^{3-}	2.350	0.003	0.794	8.170	0.109	0.999
Sr^{2+}	2.215	0.012	0.516	0.405	0.403	1.0
As^{5+}	0.735	0.009	0.427	1.365	0.975	0.760

Table 3. Removal efficiency of $NH_4^+$and PO_4^{3-} during their simultaneous adsorption for biochar dose 4 g/L

		Removal efficiency (%, RSE 0.1-0.5%)		pH after adsorption
		NH_4^+	PO_4^{3-}	
Initial ion concentration (mg/L)	10	27.1	70.0	9.68
	50	49.6	68.8	9.51
	100	55.4	68.0	9.41
	200	64.1	67.6	8.95
	300	74.4	66.7	8.90
Langmuir model	Q (mg/g)	12.392	588.2	
	b (L/mg)	0.012	0.001	
	R^2	0.915	0.118	
Freundlich model	K (L/g)	0.053	0.597	
	1/n	1.540	0.955	
	R^2	0.992	0.997	

A. Kinetics of NH_4^+, PO_4^{3-}, Sr^{2+} and As^{5+} Adsorption

The percentage of adsorption of each ion from the liquid solution by the biochar, as a function of contact time during the kinetic tests, is represented in Fig. 1. As can be clearly seen, the adsorption rate of ammonium, phosphate and strontium was fast within the first 0.5 h, removing 49.2% of ammonium, 24% of phosphate and 94.5% of strontium from the solution. The higher efficiency achieved for ammonium and strontium ions could be assigned to the negatively charged functional groups on the biochar surface, as it will be shown from the FTIR spectra below, which favor the adsorption of cations. On the other hand, the adsorption rate of arsenate was very low during this time interval, about 6%. As it will be explained later, this bahavior is attributed to the negatively charged oxyanions of As^{5+} in the solution. Equilibrium was attained in 1 h, 12 h, 3 h and 12 h for ammonium, phosphate, strontium and arsenate, respectively, with maximum adsorption efficiency of 47% for ammonium and 36% for phosphate at an initial concentration of 50 mg/L (Fig. 1a) and 99% for strontium and 29% for arsenate at an initial concentration of 10 mg/L (Fig. 1b).

The kinetic parameters calculated by applying the two models described by Eq. (2) and Eq. (3) are presented in Table 2. As can be observed, the fit of the pseudo-second-order model to the experimental data was far more successful than that of the pseudo-first model, agreeing with earlier studies [1, 13, 14, 18–20, 26]. This model reveals that the rate-limiting step between each adsorbate and adsorbent was a chemisorptions reaction.

C. Co-adsorption of NH_4^+ and PO_4^{3-}, by the Biochar at Equilibrium

The removal efficiency of ammonium and phosphate ions by the biochar, when these ions co-existed in the solution, for a range of initial concentrations, is indicated in Table 3. As can be noticed, when ammonium flux density increased its adsorption on the biochar surface was favored, reaching a maximum of 74.4% at an initial concentration of 300 mg/L. On the other hand, the uptake of phosphate peaked at a low initial concentration of 10 g/L, attaining a value of 70% and slightly declined at higher concentrations, implying the saturation of the active sites on biochar surface. The pH of the solution after adsorption, as Table 3 shows, was alkaline, varying between 8.9 and 9.68. pH is an important factor of the process, because it governs the state of the ions, their charge and the surface charge of the adsorbent. At pH values above 9 part of the ammonium was converted to NH_3 [1, 6] and the adsorption capacity was rather low. When pH was between 8 and 9, at initial concentrations higher than 100 mg/L, adsorption of ammonium was favored, due to the negatively charged surface of the adsorbent, as it will be shown below. Past investigations have shown that when the pH< 2.1 the phosphate in the solution is principally in the form of H_3PO_4, when 2.1 <pH< 7.2 it is in the form of $H_2PO_4^-$, when 7.2 <pH< 12.3 dominant species are HPO_4^{2-}, while when pH> 12.3 they exist as PO_4^{3-}. The results of Table 3 show that phosphate in current experiments was principally present in the solution in the form of HPO_4^{2-} [5]. Thus, taking into consideration that an alkaline pH could reduce the adsorption ability by repulsion, due to competition between OH^- and phosphate ions, adsorption of phosphate by the negatively charged biochar seems to occurred through ligand exchange with negative functional groups.

Based on previous results by the authors [22, 23], the uptake of ammonium or phosphate by the adsorbent increased when both ions co-existed in the solution, suggesting that there was no competition between them for sorption sites on the solid surface. The ratio of multi-ion to mono-ion adsorption efficiency was greater than unity, up to 1.3 for ammonium and 2.4 for phosphate.

In a previous work, examining the potential of date palm biochar for the simultaneous removal of ammonium and phosphate from aqueous solutions, it was found that the removal and adsorption capacities for ammonium (48 mg/g) and phosphate (27.4 mg/g) were higher in mixed solutions, agreeing with current results [13]. In contrast, the application of a sewage sludge-derived biochar to bi-solute adsorption of ammonium and phosphate ions showed that the sorption capacity for ammonium dropped from 36 mg/g, during single-solute adsorption, to 10 mg/g during bi-solute adsorption, whereas that of phosphate from 88.1 mg/g to 63.2 mg/g, respectively [15].

The characteristic parameters which were calculated by applying the Langmuir and Freundlich isotherm models, described by Eqs. (4) and (5), are also included in Table 3 for comparison. These results show that the Freundlich model fitted successfully the experimental data of simultaneous ammonium and phosphate ions adsorption on the biochar, with correlation coefficients of 0.992 and 0.997, respectively. According to the theory of the above models, both ions followed a multilayer adsorption mechanism on the adsorbent surface, through a heterogeneous process. Past investigations on concomitant adsorption of ammonium and phosphate by various biochar composite materials reported either Langmuir or Freundlich models to best describe the equilibrium isotherm data of adsorption [6, 17].

Table 4. Removal efficiency of NH_4^+, PO_4^{3-}, Sr^{2+}, As^{5+} ions during their simultaneous adsorption as a function of initial concentration and adsorbent dose

Initial ion concentration (mg/L)	Adsorbent dose 4 g/L				
	Removal efficiency ((%, RSE 0.1-0.5%)				pH after adsorption
	NH_4^+	PO_4^{3-}	Sr^{2+}	As^{5+}	
10	49.0	70.0	92.2	12.0	9.52
50	75.4	74.0	92.5	13.2	9.36
100	81.7	79.0	92.8	15.5	9.12
200	84.0	79.0	91.0	14.0	8.81
300	86.0	79.0	89.1	12.1	8.41
	Adsorbent dose 2 g/L				
10	36.5	60.0	86.5	68.4	8.81
50	64.1	73.0	87.0	68.6	8.68
100	73.3	82.0	87.6	68.1	8.48
200	76.0	81.6	86.6	75.0	8.34
300	77.6	80.7	85.6	83.9	7.98

D. Co-adsorption of NH_4^+, PO_4^{3-}, Sr^{2+} and As^{5+} by the Biochar at Equilibrium

The multi-ion adsorption experiments were conducted in order to examine whether there was a competition between them, when all four ions co-existed in the solution. The results are summarized in Table 4, which includes the removal efficiency of each ion by the biochar and the pH of the solution after adsorption, for the whole range of initial concentrations studied and for two adsorbent doses 4 g/L and 2 g/L. It can be clearly seen that for ammonium and phosphate ions, when the ionic strength was higher, the adsorption process by the available sites on the biochar surface was favored, so that at the highest initial concentration of 300 mg/L the removal efficiency reached a maximum of 86% for ammonium and 79% for phosphate (adsorbent dose 4 g/L). The same trend was observed in the case of strontium and arsenate ions, but up to concentrations of 100 mg/L. At higher values the efficiency declined, due to saturation of the biochar surface. Furthermore, Table 4 shows that when the adsorbent dose was 2 g/L the uptake of ions by the solid material was somehow lowered, with the exception of arsenate, which is also supported by past investigations [14].

The pH of the solution was alkaline throughout the process, varying between 8.41 and 9.52 for an adsorbent dose of 4 g/L and between 7.98 and 8.81 for an adsorbent dose of 2 g/L. This alkaline pH could favor the electrostatic attraction or complexation of cations NH_4^+ and Sr^{2+} on the biochar surface, which was negatively charged. On the other hand, for such pH values phosphate and arsenate species existed as HPO_4^{2-} [5] and $HAsO_4^{2-}$ [14, 20], respectively, so that the more alkaline the pH the lower the adsorption capacity by the solid surface, due to increasing competition between OH^-, HPO_4^{2-} or $HAsO_4^{2-}$ species for available sites. Also, the alkaline pH could enhance de-protonation at the solid surface, leading to more negative sites for increased adsorption of cations such as Sr^{2+} through chemical bonding, and repulsion of anions HPO_4^{2-} and $HAsO_4^{2}$. This implies that the oxyanions studied could have been adsorbed through a ligand exchange with the adsorbent surface or through chemical complexation [20, 23].

A comparison between the percentage of each ion sorbed by the biochar material (adsorbent dose 4 g/L), under conditions of multi-ion adsorption, and the corresponding one under conditions of single ion adsorption, is made in Fig. 2. These data show that the uptake of each ion by the solid increased significantly when all ions co-existed in the solution, up to 88.5% for ammonium, over 100% for phosphate and up to 89.4% for strontium. In the case of arsenate, the removal efficiency from the solution was improved, as compared to single ion adsorption, when the adsorbent dose was 2 g/L, as previously discussed. The increase in percentage adsorbed exceeded the value of 100% at low initial concentrations. Accordingly, the efficiency of adsorption from multi-ion solutions was dependent not only on the ions content, but also on their proportions on the surface of the adsorbent, so that more ions favored the process until saturation. Additionally, the fast adsorption of ammonium and strontium cations on the negatively charged char by electrostatic attraction, as previously shown, "neutralized" the solid surface to some extent, leading to reduced repulsion of oxyanions HPO_4^{2-} and $HAsO_4^{2-}$, or in other words facilitating their adsorption on the solid surface. As will be analyzed in section E, the mechanisms of adsorption of studied ions were different, besides complex, so there seemed to be no competition between ammonium, phosphate, strontium and arsenate ions for sorption sites on the biochar surface.

The simultaneous adsorption of all these ions on biochars has not been reported so far, to the best of our knowledge, which makes comparison of present results with literature data difficult. As already discussed, data on the bi-solute adsorption of ammonium and phosphate ions only showed both competitive [15] and noncompetitive [13] adsorption on agricultural or sewage sludge biochars.

The adsorption isotherms constructed upon application of the Langmuir and Freundlich models are illustrated in Fig. 3 and compared with the experimental data at equilibrium conditions, whereas the characteristic model parameters, described in the experimental section, are indicated in Table 5. From these results it is obvious that the Freundlich model, which assumes a multilayer adsorption mechanism, fitted with great accuracy the experimental data. For an adsorbent dose of 4 g/L, correlation coefficients ranged between 0.970 and 0.996, the latter corresponding to the phosphate adsorption process. For an adsorption dose of 2 g/L, R^2 values varied between 0.954 and 0.997. The best fit was obtained for strontium adsorption. When the adsorbent dose was 4 g/L, the maximum adsorption capacity of the solid for ammonium, phosphate, strontium and arsenate, co-existing in the solution, was 50.3 mg/g, 59.2 mg/g, 66.9 mg/g and 9.1 mg/g, respectively. When the adsorbent dose was halved to 2 g/L, the corresponding values for ammonium, phosphate, strontium and arsenate were 45.4 mg/g, 121 mg/g, 64.2 mg/g and 62.9 mg/g, respectively.

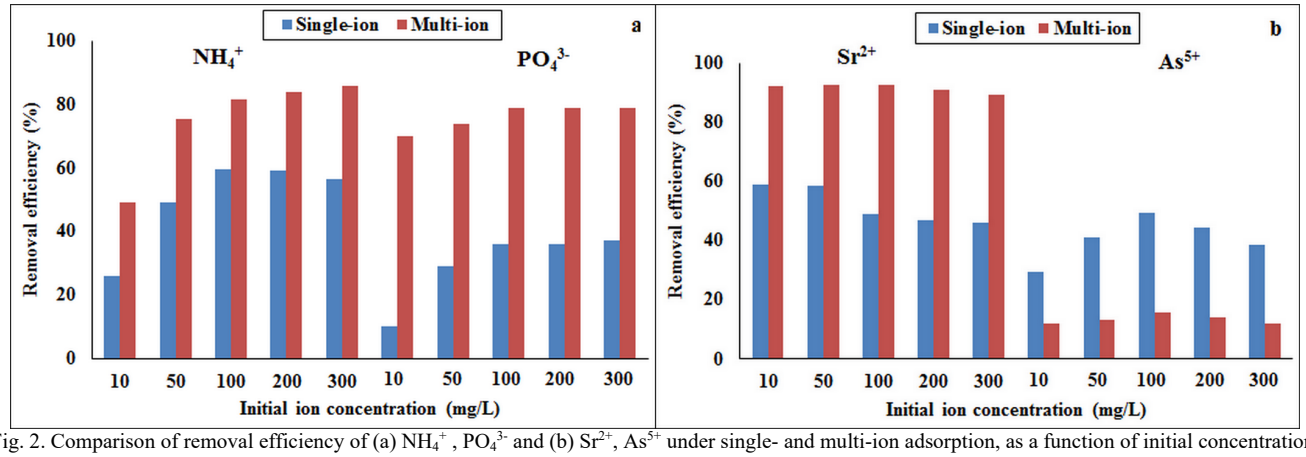

Fig. 2. Comparison of removal efficiency of (a) NH_4^+ , PO_4^{3-} and (b) Sr^{2+}, As^{5+} under single- and multi-ion adsorption, as a function of initial concentration.

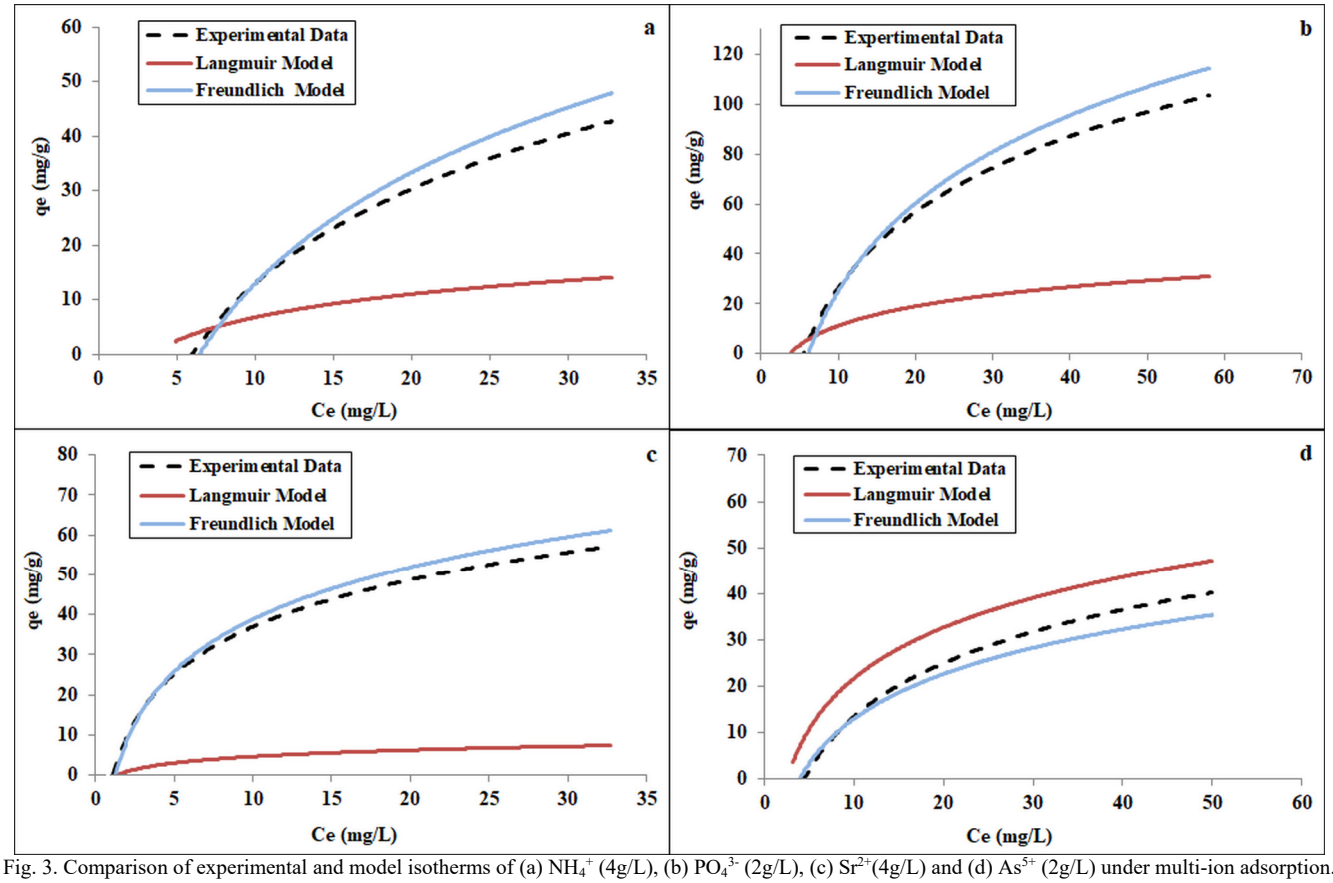

Fig. 3. Comparison of experimental and model isotherms of (a) NH_4^+ (4g/L), (b) PO_4^{3-} (2g/L), (c) Sr^{2+}(4g/L) and (d) As^{5+} (2g/L) under multi-ion adsorption.

Table 5. Isotherm model parameters of of NH_4^+, PO_4^{3-}, Sr^{2+}, As^{5+} ions under multi-ion adsorption

	Adsorbent dose 4 g/L					
	Langmuir model			Freundlich model		
	Q (mg/g)	b (L/mg)	R^2	k (L/g)	1/n	R^2
NH_4^+	40.6	0.017	0.809	0.072	1.924	0.970
PO_4^{3-}	106.4	0.006	0.596	0.489	1.172	0.996
Sr^{2+}	188.7	0.016	0.903	3.234	0.909	0.990
As^{5+}	53.5	0.426	0.362	0.034	1.026	0.992
	Adsorbent dose 2 g/L					
NH_4^+	42.4	0.010	0.687	0.041	1.824	0.974
PO_4^{3-}	83.3	0.012	0.455	0.487	1.410	0.977
Sr^{2+}	625.0	0.001	0.451	1.681	0.986	0.997
As^{5+}	99.0	0.019	0.619	0.383	1.193	0.954

These results can be compared only with those reported for similar unmodified materials for the removal of ammonium and phosphate from binary systems. Adsorption capacities achieved from such systems for ammonium and phosphate ions ranged between 10–48 mg/g and 27.4–63.2 mg/g, respectively [13, 15]. Current values are comparable or even higher than those for modified biochar materials, which varied between 0.7–177.2 mg/g for ammonium and 1.4–253.9 mg/g for phosphate, during their simultaneous adsorption [2, 3, 6–8, 16, 17]. Concerning strontium and arsenate, a comparison can only be made with adsorption data from single solutions by agricultural waste biochars, with maximum adsorption capacities ranging between 0.6 mg/g and 0.74 mg/g for strontium [18] and 0.8 mg/g and 7.1 mg/g for arsenate [19, 20].

The use of low-cost nontoxic modifiers of biochar is a future task, aiming to further increase the adsorption capacity of the "green" adsorbent under study.

E. Mechanisms of NH_4^+, PO_4^{3-}, $Sr^{2+}$and As^{5+} Simultaneous Adsorption by the Biochar

Besides ultimate analysis, structural characteristics and pH measurements during the adsorption process, FTIR and XRD analyses were conducted, before and after the adsorption of ions, in order to get a deeper understanding of the possible mechanisms, which are complex and include electrostatic attraction, ligand exchange, chemical complexation, electron coordination and surface precipitation between adsorbent and adsorbates.

Fig. 4a, representing the FTIR spectra of the solid material prior to adsorption, shows some small peaks at wave numbers 834 cm^{-1}, 876 cm^{-1} and 1006 cm^{-1} assigned to C-H bending vibration of aromatic substances, CO_3^{2-} carbonates and C=C bending of alkene groups, respectively. Stretching vibration of C=C groups from cycloalkenes also appeared at wave number 1574 cm^{-1}. All other peaks, the broader bands at 1226 cm^{-1} and 1402 cm^{-1}, as well as the sharp peak at 2350 cm^{-1}, correspond to oxygenated compounds, specifically stretching vibrations of C-O from ethers and carboxylic substances, O-H bending of alcohols and vibrational stretching of O=C=O, respectively. Therefore, almond husks biochar was enriched in negatively charged functional groups incorporating oxygen and presented increased polarity and hydrophilicity, as previously discussed. These groups could favor the adsorption of cations on the solid surface such as NH_4^+ and Sr^{2+}, through electrostatic attraction or formation of

chemical complexes.

The FTIR spectra of the material after the simultaneous adsorption of all ions from the solution, illustrated in Fig.4b, presented large differences from the one corresponding to the material before the adsorption process. The transmittance intensity was significantly higher, whereas several peaks attributed to C-H, COO^{2-}, C=C, C-O and O-H bonds from aromatic, carboxylic, alkene/cycloalkene, ether and alcohol compounds, disappeared. On the other hand, new peaks appeared in the post-adsorption spectra at wave numbers 1286 cm^{-1}, 1706 cm^{-1} and 2898/2952 cm^{-1} related to C-O, C=O and C-H/O-H stretching vibrations representative of aromatic esters, carboxylic acid and alkanes/alcohols, respectively. This implies that interactions occurred between the ions adsorbed and the above functional groups through chemical complexation. Also, the new sharp peak at 1224 cm^{-1} and the broad band at 1538 cm^{-1}, assigned to vibrational stretching of amines (C-N) and nitro-compounds (N-O), indicate adsorbed ammonium-formed complexes on biochar's surface. Additionally, the new 1058 cm^{-1} peak shows that phosphate was adsorbed via complexation with oxygen-containing functional groups on the solid surface (P-O bond). Finally, current results suggest that, as the pH of the solution was found to be alkaline during the process and oxyanions HPO_4^{2-} and $HAsO_4^{2-}$ were significantly adsorbed by the biochar, these could have interacted with O-H groups onto the adsorbent surface via a ligand exchange mechanism. Such mechanisms have also been reported by previous studies [1, 11, 19].

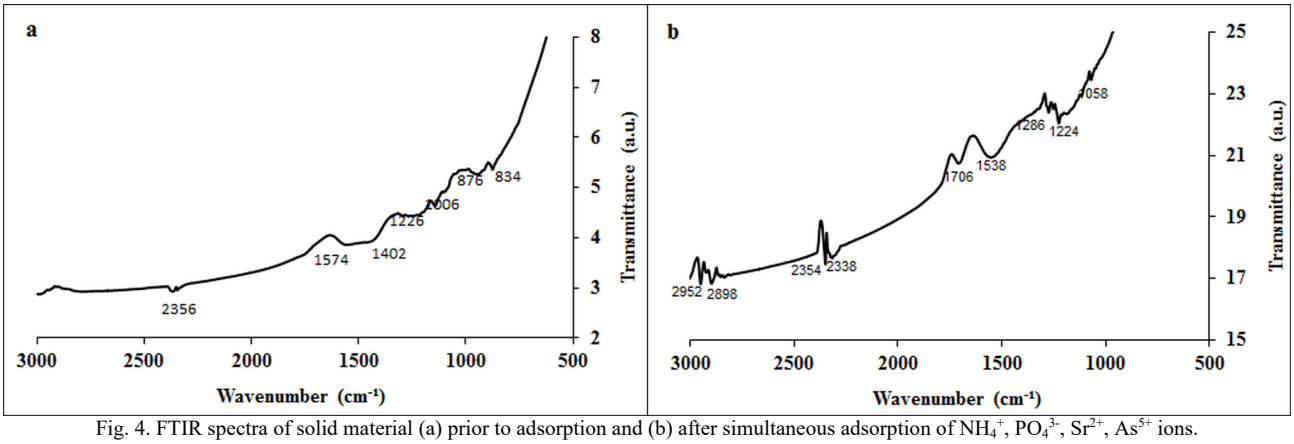

Fig. 4. FTIR spectra of solid material (a) prior to adsorption and (b) after simultaneous adsorption of NH_4^+, PO_4^{3-}, Sr^{2+}, As^{5+} ions.

To prove whether precipitation occurred during the adsorption process, the XRD spectra of the biochar material, prior to and after the adsorption of ions were studied. Surface precipitation is an important mechanism for solid adsorbents to remove various ions from a contaminated solution. In this process, metals, mineral phases or other chemical groups on the solid surface can form stable inorganic precipitates with some ions of the aqueous solution. Interpreting the spectra in Fig. A2 is challenging, due to the amorphous carbon content of the biochar, but several key inorganic species were identified. The principal mineral phases of the original material were calcite and arcanite, indicating that this was enriched in Ca and K. Hydroxylapatite appeared in a considerable amount, due to the P content in the biochar, while quartz, niter, magnesioferrite and kalsilite, incorporating Si, K, Mg, Fe and Al were identified in small amounts.

Following the adsorption of ammonium, phosphate, strontium and arsenate ions new diffraction peaks were observed, corresponding to the mineral phases chopinite ($(Mg,Fe)_3(PO_4)_2$), newberyite ($Mg(PO_3OH).3H_2O$), strontianite ($SrCO_3$) and As-hydroxylapatite ($(Ca_5P_{2.27}As_{0.73}O_4)_3OH$). This suggests that phosphate-formed crystalline precipitates with Mg^{2+} of biochar and CO_3^{2-}, OH^- anions released from the biochar (as presented in the FTIR spectra) interacted with Sr^{2+} and As^{5+} heavy metals, resulting in the formation of mineral precipitates on the surface. Therefore, the adsorption efficiency of phosphate, strontium and arsenate ions was also improved by the precipitation process.

Based on this analysis, it can be inferred that the mechanisms involved in the immobilization of the ions studied include chemical complexation between the ions and the functional groups on the biochar surface, electrostatic attraction for ammonium and strontium cations, ligand exchange for phosphate and arsenate ions and precipitation of minerals on the solid surface for phosphate, strontium and arsenate ions.

F. Desorption of NH_4^+, PO_4^{3-}, $Sr^{2+}$and As^{5+} from the Biochar

The desorption experiments were conducted in order to assess the stability of the biochar studied and the rate of release of adsorbed metal ions or nutrients, such as N and P species, upon agricultural application of the biochar to the soil. Fig. 5 presents the leaching rate of the ions from spent biochar, after their simultaneous adsorption, as a function of time. As can be observed, desorption of ammonium and phosphate was faster during the first 12 h, releasing 3.2% of ammonium and 7.9% of phosphate. Desorption increased at a relatively slower leaching rate thereafter, attaining a value of 9.4% for ammonium and 10.7% for phosphate after 72 h. Such values are in agreement with desorption rates reported for other biochar adsorbents [6, 13, 17]. The decrease in desorption with time was attributed to the efficient binding of the ions to the solid by the mechanisms previously described. Furthermore, Fig. 5 shows that the retention of ammonium by the biochar was better than that of phosphate, implying that ammonium formed stronger bonds on the adsorbent surface by electrostatic attraction or chemical complexation. Toxic heavy metals strontium and arsenic could not be measured in the leachates for the time interval studied, which is advantageous for wastewater purification applications. This finding is verified by the mineral precipitates strontianite and As-hydroxylapatite identified from the XRD analysis, which

are practically insoluble in water. If the concentration of these metals in the biochar after adsorption justifies their recovery for various uses, then methods such as acid extraction are required. In conclusion, current results show that almond husks biochar after co-adsorption of ammonium, phosphate, strontium and arsenate can be used as a slow-release fertilizer for soil improvement.

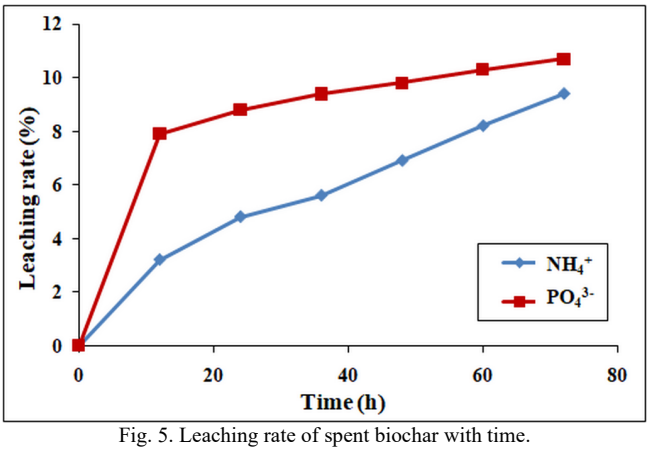

Fig. 5. Leaching rate of spent biochar with time.

G. Large-Scale Application and Future Prospects

The study herein demonstrated a high adsorption potential of ammonium, phosphate, strontium and arsenate ions by an almond husks biochar, the slow desorption of nutrients N and P, while the stable retention of toxic heavy metals strontium and arsenic by the solid. Therefore, the physical activation of the raw material is a promising method for reducing not only water pollution, but also for providing nutrients to the soil.

The experiments were conducted under controlled conditions on a lab scale, which may not fully simulate the real wastewater applications. Contaminated waters contain several impurities such as metals, inorganic ions and organic substances, which may interfere with the adsorption of specific ions. Thus, further trials with real wastewater and pilot-scale experiments are required prior to industrial applications, in order to evaluate the sustainability of the process.

The readily available waste material used in this work suggests its viability for large-scale applications. The use of spent biochar as a soil fertilizer, integrated with the use of the energy generated by the bio-oil and gases during the thermal treatment of the raw material for the requirements of the process, can significantly reduce the regeneration cost of the adsorbent. Other important issues to be studied are the optimization of all parameters involved during the adsorption process, accompanied by factorial and statistical analysis, as well as the investigation of a low-cost non toxic modifier, in order to increase the adsorption capacity.

IV. Conclusions

The almond husks biochar studied had a large specific surface area, was highly oxygenated and its surface was negatively charged. During the simultaneous adsorption of ammonium, phosphate, strontium and arsenate ions the adsorption rate of ammonium, phosphate and strontium was fast within 0.5 h, in contrast to that of arsenate. At equilibrium, a higher ionic strength favored the adsorption process by the biochar available sites, whereas the uptake of each ion by the solid increased significantly when all ions co-existed in the solution, implying no competition between them for sorption sites. The experimental data were fitted with great accuracy by the Freundlich isotherm model. The maximum adsorption capacity of the biochar achieved for ammonium, phosphate, strontium and arsenate was 50.3 mg/g, 121 mg/g, 66.9 mg/g and 62.9 mg/g, respectively. By performing ultimate and structural analyses, pH measurements, FTIR and XRD analyses, before and after the adsorption process, it was concluded that the potential mechanisms of adsorption were chemical complexation of all ions with the adsorbent, electrostatic attraction for ammonium and strontium cations, ligand exchange for phosphate and arsenate ions and mineral surface precipitation for phosphate, strontium and arsenate ions.

Appendix

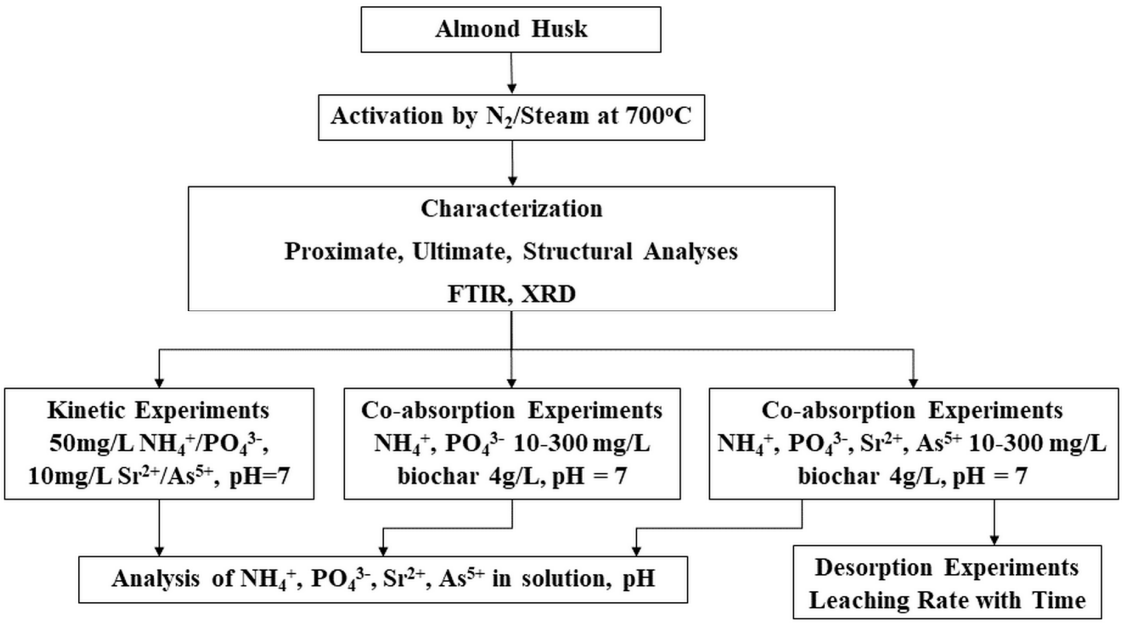

Fig. A1. Flow diagram of experimental procedure.

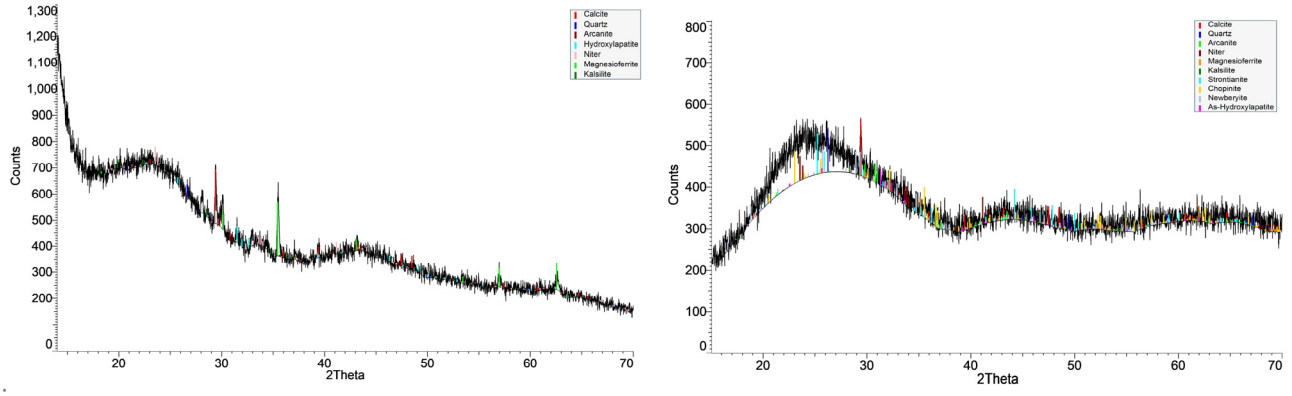

(a) (b)

Fig. A2. XRD spectra of solid material (a) prior to adsorption and (b) after simultaneous adsorption of all ions.

Conflict of Interest

The authors declare no conflict of interest.

Author Contributions

DV conceptualization, writing, supervision; GA experiments, software; AS XRD analyses, software; DP validation; all authors had approved the final version.

Acknowledgment

The authors kindly thank the laboratories of Hydrocarbons Chemistry and Hydrogeochemical Engineering and Soil Remediation of the Technical University of Crete, for the ultimate and FTIR analyses, Dr. T. Ioannides and Dr. M. Smyrnioti from the Inst. of Chemical Engineering Sciences in Patra for the BET measurements of the samples.

References

[1] V. Nguyen, T, Vo, T. Tran, T. Nguyen, T. Le, X. Bui, and L. Bach, "Biochar derived from the spent coffee ground for ammonium adsorption from aqueous solution," *Case Studies in Chem. Environ. Eng*., vol. 4, 100141, 2021.

[2] H. Li, Y. Wang, Y. Zhao, L. Wang, J. Feng and F. Sun, "Efficient simultaneous phosphate and ammonia adsorption using magnesium-modified biochar beads and their recovery performance," *J. Environ. Chem. Eng*., vol. 11, 110875, 2023.

[3] Z. Huang, B. Chang, Y. Tang, Q. Li, Z. Zhang, S. Wei *et al.*, "Co-adsorption performance and mechanisms of ammonium and phosphate by iron-modified biochar in water," *J. Water Process Eng*., vol. 67, 106209, 2024.

[4] Q. Yu, D. Xia, H. Li, L. Ke, Y. Wang, Y. Zheng, and Q. Li, "Effectiveness and mechanisms of ammonium adsorption on biochars derived from biogas residues," *RSC Adv.,* vol. 6, no. 91, pp. 88373–88381, 2016.

[5] D. Jiang, B. Chu, Y. Amano, and M. Machida, "Removal and recovery of phosphate from water by Mg-laden biochar: Batch and column studies," *Colloids Surfaces A,* vol. 558, pp. 429–437, 2018.

[6] Q. Feng, M. Chen, P. Wu, X. Zhang, S. Wang, Z. Yu, and B. Wang, "Simultaneous reclaiming phosphate and ammonium from aqueous solutions by calcium alginate-biochar composite: Sorption performance and governing mechanisms," *Chem. Eng. J*., vol. 429, 132166, 2022.

[7] B. Biswas, S. Adhikari, H. Jahromi, M. Ammar, J. Baltrusaitis, A. Torbert et al., "Magnesium doped biochar for simultaneous adsorption of phosphate and nitrogen ions from aqueous solution," *Chemosphere,* vol. 358, 142130, 2024.

[8] U. Shaheen, Z. Ye, O.K. Abass, D. Zamel, A. Rehman, P. Zhao, and F. Huang, "Evaluation of potential adsorbents for simultaneous adsorption of phosphate and ammonium at low concentrations". *Micropor. Mesopor. Materials*, vol. 379, 113301, 2024.

[9] A. Herath, C. Layne, F. Perez, E. Hassan, C. Jr Piiman, and T. Mlsna, "KOH-activated high surface area Douglas Fir biochar for adsorbing aqueous Cr(VI), Pb(II) and Cd(II)," *Chemosphere*, vol. 269, 128409, 2021.

[10] J. Liu, Z. Huang, Z. Chen, J. Sun, Y. Gao, and E. Wu, "Resource utilization of swine sludge to prepare modified biochar adsorbent for the efficient removal of Pb(II) from water," *J. Clean. Prod*., vol. 257, 120322, 2020.

[11] J. Jang, W. Miran, S. Divine, M. Nawaz, A. Shahzad, S. Woo, and D. Lee, "Rice straw-based biochar beads for the removal of radioactive strontium from aqueous solution," *Sci. Tot. Environ*., vol. 615, pp. 698–707, 2018.

[12] J. Li, B. Li, H. Huang, X. Lv, N. Zhao, G. Guo, and D. Zhang, "Removal of phosphate from aqueous solution by dolomite-modified biochar derived from urban dewatered sewage sludge," *Sci. Tot. Environ*., vol. 687, pp. 460–469, 2019.

[13] Y.H. Fseha, B. Sizirici, and I. Yildiz, "The potential of date palm waste biochar for single and simultaneous removal of ammonium and phosphate from aqueous solutions," *J. Environ. Chem. Eng.,* vol. 9, 106598, 2021.

[14] Q. Li, W. Liang, F. Liu, G. Wang, J. Wan, W. Zhang, C. Peng, and J. Yang, "Simultaneous immobilization of arsenic, lead and cadmium by magnesium-aluminum modified biochar in mining soil," *J. Environ. Manag*., vol. 310, 114792, 2022.

[15] M. Konczak, and M. Huber, "Application of the engineered sewage sludge-derived biochar to minimize water eutrophication by removal of ammonium and phosphate ions from water," *J. Clean. Prod*., vol. 331, 129994, 2022.

[16] Q. Yin, R. Wang, and Z. Zhao, "Application of Mg-Al-modified biochar for simultaneous removal of ammonium, nitrate and phosphate from eutrophic water," *J. Clean. Prod*., vol. 176, pp. 230–240, 2018.

[17] H. Xi, X. Zhang, A.H. Zhang, F. Guo, Y. Yang, Z. Lu, et al., "Concurrent removal of phosphate and ammonium from wastewater for utilization using Mg-doped biochar/bentonite composite beads," *Separat. Purific. Technol*., vol. 285, 120399, 2022.

[18] V. Chakraborty, P. Das, and P. Roy, "Carbonaceous materials synthesized from thermally treated waste materials and its application for the treatment of strontium metal solution: Batch and optimization using Response Surface Methodology," *Environ. Technol. Innov.*, vol. 15, 100394, 2019.

[19] S. Banerjee, S. Mukherjee, A. LaminKa-Ot, S.R. Joshi, T. Mandal, and G. Halder, "Biosorptive uptake of Fe^{2+}, Cu^{2+} and As^{5+} by activated biochar derived from Colocasia esculenta: Isotherm, kinetics, thermodynamics and cost estimation," *J. Adv. Res.,* vol. 7, pp. 597–610, 2016.

[20] G.J.F. Cruz, D. Mondal, J. Rimaycuna, K. Soukup, M.M. Gomez, J.L. Solis, and J. Lang, "Agrowaste derived biochars impregnated with ZnO for removal of arsenic and lead in water," *J. Environ. Chem. Eng*., vol. 8*,* 103800, 2020.

[21] D. Vamvuka, S. Alexandrakis, G. Alevizos, and A. Stratakis, "Recycling of waste materials for stabilizing ash from co-combustion of municipal solid wastes with an olive by-product: Soil leaching experiments," *Soil Systems*, vol. 4, no. 2, pp. 34-49, 2020.

[22] D. Vamvuka, E. Loupasis, E. Chamilaki, and E. Sdoukou, "Adsorption of ammonium from wastewaters by an almond kernel derived biochar modified by potassium hydroxide or dolomite and activated by steam," vol. 15, 100465, 2024.

[23] D. Vamvuka, K. Stergiou, E. Sdoukou, and A. Stratakis, "Magnesium or bentonite modified almond kernel biochar for phosphate adsorption from contaminated waster solutions," *J. Environ. Chem. Eng*., vol. 12, 111907, 2024.

[24] D. Vamvuka, D. Pentari, V. Stathopoulou and E. Sdoukou, "Physically activated nut residues as strontium and manganese adsorbents from contaminated waters-Equilibrium and isotherm models," J. Multidisc. Eng. Sci. Studies, vol. 9, no. 4, pp. 1–9, 2023.

[25] M. Jiang, Y. Yang, T. Lei, Z. Ye, S. Huang, X. Fu, et al., "Removal of phosphate by a novel activated sewage sludge biochar: Equilibrium, kinetic and mechanism studies," *Applic. Ener. Comb. Sci,* vol. 9, 100056, 2022.

[26] K. Z. Elwakeel, M. M. Ahmed, A. Akhdhar, H. M. Alghamdi, M. G. M. Sulaiman, M. Hamza and Z. A. Khan, "Effect of the magnetic core in the aliginate/gum composite on adsorption of bivalent copper, cadmium and lead ions in the aqueous system," *Int. J. Biol. Macromol*., vol. 253, 126884, 2023.